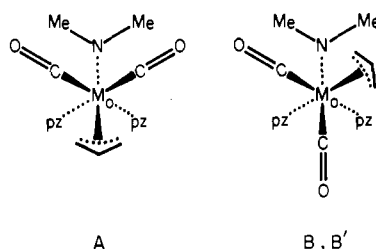


**Figure 1.** Variable-temperature  $^1\text{H}$  NMR spectrum of  $(\text{pz})\text{B}(\mu\text{-pz})_2(\mu\text{-NMe}_2)\text{Mo}(\text{CO})_2(\eta^3\text{-CH}_2\text{CHCH}_2)$ .

can see that three rotamers should exist, i.e., A, B, and its mirror image B', with B and B' having identical chemical shifts. As-



suming statistical distribution of these rotamers at low temperature ( $1/3$  A,  $2/3$  B + B'), one should observe (a) three Me peaks of equal intensity, (b) four pz 4-H peaks in  $1:2/3:2/3:2/3$  ratio corresponding to the uncoordinated pz group, the two identical coordinated pz groups in rotamer A, and the two dissimilar coordinated pz groups in B and B', (c) three different environments for the syn and anti protons of the  $\eta^3$ -allyl group. All these features are indeed observed in the low-temperature spectrum, e.g., the three sharp Me signals near 2.6–2.2 ppm and the pz 4-H peaks in the 6.5–6.2 ppm range.

There are only very minor differences in the  $^1\text{H}$  NMR spectrum of  $(\text{pz})\text{B}(\mu\text{-pz})_2(\mu\text{-NMe}_2)\text{Mo}(\text{CO})_2(\eta^3\text{-CH}_2\text{CCH}_3\text{CH}_2)$  over the range +60 to  $-44^\circ\text{C}$ . On the basis of selective-decoupling experiments (and in agreement with the intensity measurements), the signals  $\delta(^1\text{H}) = 7.88/7.76/6.46$  are readily assigned to the lone terminal pz group.

The reason for  $\text{L}^*$  coordinating as it does, instead of as  $\text{Me}_2\text{NB}(\mu\text{-pz})_3$ , resides probably in the stronger nucleophilicity of the  $\text{NMe}_2$  group vs. pz (since the lone pair of the  $\text{NMe}_2$  nitrogen is not donating to boron); it may also be favored by the greater compactness of the molecule where the  $\text{B}(\mu\text{-pz})_2\text{Mo}$  ring is further bridged by a single atom.

### Experimental Section

Elemental analyses were performed by the Schwarzkopf Microanalytical Laboratory, Woodside, NY; the compounds gave satisfactory data. Melting points (uncorrected) were determined on a Mel-Temp block.

NMR spectra were recorded on a Varian XL-200 instrument. Chemical shift data are given in ppm with positive values indicating downfield shifts from the reference (internal  $\text{Me}_4\text{Si}$  for  $^1\text{H}$ ; external  $\text{Et}_2\text{O}\cdot\text{BF}_3$  for  $^{11}\text{B}$ ); s = singlet, d = doublet, t = triplet, and an asterisk denotes a broad signal. Coupling constants  $J$  are given in Hz.

**$\text{Li}[\text{Me}_2\text{NB}(\text{pz})_3]$ .** A solution of methyllithium in ether (10 mL of a 1.8 M solution) was added dropwise with stirring to a mixture of 2.5 g (9.7 mmol) of dimethylamine-tris(1-pyrazolyl)borane<sup>2</sup> and 20 mL of

benzene. Gas evolution started immediately with slight warming of the reaction mixture. After complete addition, the mixture was stirred at ambient temperature for 3 h. The precipitate was collected and washed with benzene and hexane to yield 2.2 g (86%) of the desired compound; it began, on heating, to decompose near  $130^\circ\text{C}$ .

NMR data (solution in  $\text{Me}_2\text{SO}-d_6$ ):  $\delta(^1\text{H}) = 7.48$  (1 H, d,  $J = 1.2$ ), 7.20 (1 H, d,  $J = 1.9$ ), 6.10 (1 H, t,  $J = 1.7$ ), 2.08 (2 H, s);  $\delta(^{11}\text{B}) = +2.7$  ( $h_{1/2} = 140$  Hz).

**$\text{pzB}(\mu\text{-pz})_2(\mu\text{-NMe}_2)\text{Mo}(\text{CO})_2(\eta^3\text{-CH}_2\text{CCH}_3\text{CH}_2)$ .** A mixture of 2.56 g (10 mmol) of (dimethylamine)-tris(1-pyrazolyl)borane<sup>2</sup> and 3.25 g (10 mmol) of freshly prepared  $(\text{MeCN})_2\text{Mo}(\text{CO})_2\text{Cl}(\eta^3\text{-CH}_2\text{CCH}_3\text{CH}_2)$ <sup>5</sup> was stirred overnight in 50 mL of methylene chloride. The solution was shaken with water, and the organic layer was chromatographed on alumina packing and eluted with cyclohexane. Evaporation of the solvent gave 3.4 g (74%) of a yellow residue, which was recrystallized from heptane; mp  $141\text{--}142^\circ\text{C}$ .

NMR data are as follows. For solution in  $\text{CD}_3\text{CN}$ :  $\delta(^1\text{H}) = 7.96$  (2 H, d,  $J = 1.9$ ), 7.90 (2 H, d,  $J = 1.9$ ), 7.88 (1 H, d,  $J \approx 1.5$ ), 7.76 (1 H, d,  $J \approx 1.5$ ), 6.46 (1 H, unsym t = two overlapping d,  $J \approx 1.3$ ), 6.31 (2 H, t,  $J = 2.2$ ), 3.50 (2 H, s), 2.48\* (6 H, s), 1.83 (3 H, s), 1.14 (2 H, t);  $\delta(^{11}\text{B}) = +2.4$  (s,  $h_{1/2} = 25$  Hz). At  $60^\circ\text{C}$ :  $\delta(^1\text{H}) = 7.94$  (2 H, d), 7.87 (3 H, 2 overlapping d), 7.74 (1 H, d), 6.45 (1 H, unsym t = 2 overlapping d), 6.30 (2 H, t), 3.49 (2 H, s), 2.50\* (6 H, s), 1.84 (3 H, s), 1.14 (2 H, s). At  $-44^\circ\text{C}$ :  $\delta(^1\text{H}) = 7.98$  (2 H, d), 7.95 (2 H, d), 7.91 (1 H, d), 7.79 (1 H, d), 6.48 (1 H, unsym t = two overlapping d), 6.34 (2 H, t), 3.51 (2 H, s), 2.49 (small s), +2.43 (6 H, s), 1.81 (3 H, s), 1.14 (2 H, s), 1.14 (2 H, s).

**$\text{pzB}(\mu\text{-pz})_2(\mu\text{-NMe}_2)\text{Mo}(\text{CO})_2(\eta^3\text{-CH}_2\text{CHCH}_2)$**  was prepared in a fashion analogous to that described for the preceding compound using  $(\text{MeCN})_2\text{MoBr}(\text{CO})_2(\eta^3\text{-CH}_2\text{CHCH}_2)$ .<sup>5</sup> The desired compound was obtained in 67% yield; mp (after recrystallization from heptane)  $122\text{--}123^\circ\text{C}$ .

NMR data (solution in  $\text{CDCl}_3$ ;  $25^\circ\text{C}$ ):  $\delta(^1\text{H}) = \text{ca. } 8.0\text{--}7.5$  (1 H, very very broad), 7.85 (2 H, d,  $J = 2.3$ ), 7.80 (1 H, d,  $J = 1.5$ ), 7.75 (2 H, d,  $J = 2.2$ ), 6.44 (1 H, t,  $J = 2.1$ ), 6.25 (2 H, unresolved t), 3.41\* (3 H, very broad unresolved m), 2.18\* (6 H, very broad s), 1.39 (2 H, d,  $J \approx 8$ );  $\delta(^{11}\text{B}) = +2.7$  ( $h_{1/2} = 30$  Hz). For additional  $^1\text{H}$  NMR data see Figure 1.

**Acknowledgment.** This work was supported by the Office of Naval Research (K.N.).

**Registry No.**  $\text{Li}[\text{Me}_2\text{NB}(\text{pz})_3]$ , 98839-65-7;  $\text{pzB}(\mu\text{-pz})_2(\mu\text{-NMe}_2)\text{Mo}(\text{CO})_2(\eta^3\text{-CH}_2\text{CCH}_3\text{CH}_2)$ , 98839-66-8;  $\text{pzB}(\mu\text{-pz})_2(\mu\text{-NMe}_2)\text{Mo}(\text{CO})_2(\eta^3\text{-CH}_2\text{CHCH}_2)$ , 98839-67-9;  $\text{Me}_2\text{HN}\cdot\text{B}(\text{pz})_3$ , 81004-03-7;  $(\text{MeCN})_2\text{Mo}(\text{CO})_2\text{Cl}(\eta^3\text{-CH}_2\text{CCH}_3\text{CH}_2)$ , 97590-30-2;  $(\text{MeCN})_2\text{MoBr}(\text{CO})_2(\eta^3\text{-CH}_2\text{CHCH}_2)$ , 33221-76-0.

(5) Hayter, R. G. *J. Organomet. Chem.* **1968**, *13*, P1–P3.

Contribution from the Department of Chemistry, Technion-Israel Institute of Technology, Haifa 32000, Israel

### Phosphato Complexes of Pentaammineruthenium

Yigal Ilan

Received June 5, 1985

The  $(\text{NH}_3)_5\text{Ru}^{\text{II/III}}$  moiety has been utilized recently to study molecules of biological interest. It was attached to several metalloproteins in order to study electron transfer to the metal centers of these molecules,<sup>1,2</sup> and to other proteins, as a probe of their structure and properties.<sup>3,4</sup> Attempts have also been made to

(1) Thompson, J. S.; Zitzmann, J. L.; Marks, T. J.; Ibers, J. A. *Inorg. Chim. Acta* **1980**, *46*, L101–L105.  
 (2) Niedenzu, K.; Seelig, S. S.; Weber, W. Z. *Anorg. Allg. Chem.* **1981**, *483*, 51–62.  
 (3) Trofimenko, S. *J. Am. Chem. Soc.* **1969**, *91*, 3183–3189.  
 (4) Meakin, P.; Trofimenko, S.; Jesson, J. P. *J. Am. Chem. Soc.* **1972**, *94*, 5677–5681.

(1) (a) Nocera, D. G.; Winkler, J. R.; Yocum, K. M.; Bordignon, E.; Gray, H. B. *J. Am. Chem. Soc.* **1984**, *106*, 5145–5150 and references therein.  
 (b) Margalit, R.; Pecht, I.; Gray, H. B. *J. Am. Chem. Soc.* **1983**, *105*, 301–302. (c) Kostic, N. M.; Margalit, R.; Che, C.-M.; Gray, H. B. *J. Am. Chem. Soc.* **1983**, *105*, 7765–7767. (d) Crutchley, R. J.; Ellis, W. R., Jr.; Gray, H. B. *J. Am. Chem. Soc.* **1985**, *107*, 5002–5004.  
 (2) (a) Isied, S. S.; Kuehn, C. G.; Worosila, G. *J. Am. Chem. Soc.* **1984**, *106*, 1722–1726 and references therein. (b) Isied, S. S. *Prog. Inorg. Chem.* **1984**, *32*, 443–517.

**Table I.** Spectral Features and  $pK_a$  Values of Pentaammineruthenium(III)-Phosphato Complex Ions

complex ion	$\lambda_{max}$ , nm	$\epsilon_{max}$ , $10^3$ $M^{-1} cm^{-1}$	$pK_a$
$[(NH_3)_5Ru^{III}(H_3PO_4)]^{3+ a}$	269, 227	1.0, 1.05	$\sim -1$
$[(NH_3)_5Ru^{III}(H_2PO_4)]^{2+ b}$	281	1.7	3.3
$[(NH_3)_5Ru^{III}(HPO_4)]^{+ c}$	304	1.9	8.3
$[(NH_3)_5Ru^{III}(PO_4)]^{0 d}$	336, 240 (sh)	2.2	

<sup>a</sup> 70% HClO<sub>4</sub> (11.6 M). The spectrum showed almost no change between 0.1 and 1 M CF<sub>3</sub>SO<sub>3</sub>H, a very significant change between 1 and 6 M CF<sub>3</sub>SO<sub>3</sub>H, and a slight change between 6 M CF<sub>3</sub>SO<sub>3</sub>H and 11.6 M HClO<sub>4</sub>. <sup>b</sup> 0.1 M CF<sub>3</sub>SO<sub>3</sub>H. <sup>c</sup> 0.1 M KH<sub>2</sub>PO<sub>4</sub>/KOH buffer, pH 6.5. <sup>d</sup> 0.1 M K<sub>2</sub>HPO<sub>4</sub>, pH 10.5 (adjusted with KOH).

design anticancer pharmaceuticals based on ruthenium complexes, exploiting the different kinetic labilities and thermodynamic affinities toward ligands of the two easily interchangeable oxidation states of ruthenium—Ru(III) and Ru(II).<sup>5</sup>

These studies are carried out in aqueous solution in the physiological pH range, and phosphate buffer is used to maintain the pH. Phosphate is of course present in the *in vivo* systems, as well.

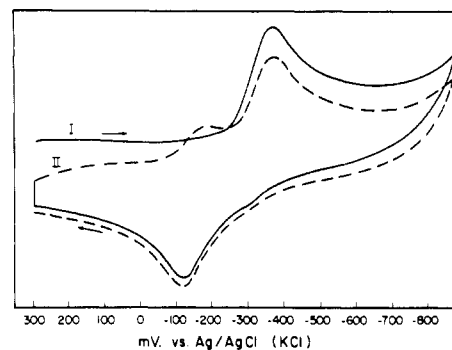
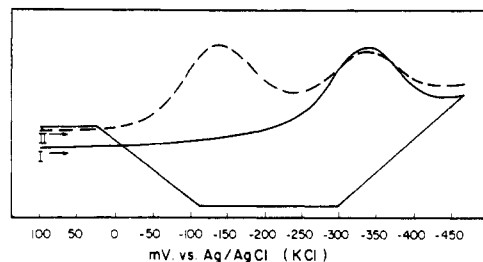
Ru(III) shows high affinity toward ligands that are hard bases, such as halides and carboxylates.<sup>6</sup> It is therefore expected that Ru(III) will also have a high affinity toward phosphate anions. In fact, an indication to that effect has been mentioned recently.<sup>7</sup>

Reactions of the kinetically inert Ru(III) ion are catalyzed by the relatively labile Ru(II) ion.<sup>6</sup> Ru(II) species are produced at neutral pH and above, by way of ligand oxidation and disproportionation. Ru(III) was shown to oxidize ammine ligands coordinated to it,<sup>8</sup> the product of this reaction being an imine bound to Ru(II). The pyridine complex of pentaammineruthenium(III) undergoes disproportionation in slightly basic pH to the Ru(II) and Ru(IV) oxidation states.<sup>9</sup> A similar disproportionation reaction in slightly basic pH (>8) was observed with (NH<sub>3</sub>)<sub>4</sub>Ru<sup>III</sup> chelated by deprotonated 2-(1-hydroxyethyl)pyridine.<sup>10</sup> The Ru(II) products of these reactions are stabilized by back-donation of electrons from the  $t_{2g}$  orbitals of Ru(II), which have  $\pi$  symmetry to  $\pi^*$  orbitals of the ligands.

We have encountered formation of phosphate-bound Ru(III) ammine species in studies of glycylamide, glycylglycine, and their derivatives bound to Ru(III) through the amino nitrogen and the amido oxygen,<sup>11</sup> at neutral and slightly basic pH—conditions which favor production of Ru(II)-bound oxidation products of the amino group.<sup>12</sup>

In the present work it has been undertaken to characterize the products of this interaction, in order to be able to understand fully systems that comprise both ruthenium ammine ions and phosphato species.

$[(NH_3)_5Ru(H_2PO_4)](PF_6)_2 \cdot 2H_2O$ <sup>13</sup> was prepared by employing the principles used by Stritar and Taube<sup>6</sup> for the preparation of pentammineruthenium(III) carboxylato complexes; namely, substitution on Ru(III) was catalyzed by Ru(II). A 250-mg sample of (NH<sub>3</sub>)<sub>5</sub>Ru(CF<sub>3</sub>SO<sub>3</sub>)<sub>3</sub><sup>14</sup> was dissolved in 3 mL of 1 M

**Figure 1.** Cyclic voltammogram of  $[(NH_3)_5Ru^{III}(H_2PO_4)]^{2+}$  in 0.1 M KH<sub>2</sub>PO<sub>4</sub> (pH 4.1, scan rate 0.1 V s<sup>-1</sup>): I, first scan; II, second scan.**Figure 2.** Square-wave voltammogram of  $[(NH_3)_5Ru^{III}(H_2PO_4)]^{2+}$  in 0.1 M KH<sub>2</sub>PO<sub>4</sub> (pH 4.1, scan rate 0.1 V s<sup>-1</sup>): I, first scan; II, second scan.

NaH<sub>2</sub>PO<sub>4</sub>, in a 10-mL beaker. The pH was adjusted to 5.0–5.4 with concentrated NaOH, and a catalytic amount of Ru(II) was generated by adding zinc amalgam to the aerated solution. The solution was stirred for  $\sim 10$  min, after which the amalgam was removed. The yellow solution was stirred for several more minutes and then filtered. The pH was adjusted to  $\sim 1.5$  with distilled CF<sub>3</sub>SO<sub>3</sub>H, and  $[(NH_3)_5Ru(H_2PO_4)](PF_6)_2 \cdot 2H_2O$  was precipitated by adding  $\sim 1.5$  g of solid NH<sub>4</sub>PF<sub>6</sub> to the filtrate. Precipitation commenced immediately, but the solution was cooled in ice for a higher yield. The yield was 0.123 g (51%).

The pentaammineruthenium(III) phosphato species were characterized by UV spectroscopy. The spectral features of the species in their various degrees of protonation are given in Table I, together with their  $pK_a$  values. The  $pK_a$  values of the mono- and diprotonated species were determined by spectrophotometric titrations.<sup>17</sup>

The spectral features are similar to those of other Ru(III) complexes in which ligands are bound to the metal center by an oxygen atom, such as carboxylates,<sup>6</sup> hydroxide,<sup>6</sup> and oxygen-bound amides.<sup>11</sup> The absorption peaks shift to lower energy as the ligand becomes more highly charged upon deprotonation. This is in accord with the ligand to metal charge-transfer character of this absorption.

The electrochemical behavior of the phosphato complex was studied by using cyclic voltammetry, square-wave voltammetry<sup>18</sup> (both using a carbon-paste working electrode), and conventional polarography (at a dropping-mercury electrode).<sup>19</sup> The first scan

- (3) Recchia, J.; Matthews, C. R.; Rhee, M.; Horrocks, W. D., Jr. *Biochim. Biophys. Acta* **1982**, *702*, 105–111.  
 (4) Matthews, C. R.; Erickson, P. M.; Froebe, C. L. *Biochim. Biophys. Acta* **1980**, *624*, 499–510.  
 (5) Clarke, M. J. "Metal Ions in Biological Systems"; Siegel, H., Ed.; Marcel Dekker: New York, 1980; vol. 11, pp 231–283.  
 (6) Stritar, J. A.; Taube, H. *Inorg. Chem.* **1969**, *8*, 2281–2292.  
 (7) Diamantis, A. A.; Murphy, W. R.; Meyer, T. J. *Inorg. Chem.* **1984**, *23*, 3230–3234.  
 (8) Diamond, S. E.; Tom, G. M.; Taube, H. *J. Am. Chem. Soc.* **1975**, *97*, 2661–2664.  
 (9) Rudd, DeF. P.; Taube, H. *Inorg. Chem.* **1971**, *10*, 1543–1544.  
 (10) Tovrog, B. S.; Diamond, S. E.; Mares, F. *J. Am. Chem. Soc.* **1979**, *101*, 5067–5069.  
 (11) (a) Ilan, Y.; Taube, H. *Inorg. Chem.* **1983**, *22*, 1655–1664. (b) Ilan, Y.; Taube, H. *Inorg. Chem.* **1983**, *22*, 3144–3151.  
 (12) Ilan, Y., unpublished results.  
 (13) Anal. Calcd for H<sub>21</sub>F<sub>12</sub>N<sub>5</sub>O<sub>6</sub>P<sub>3</sub>Ru: H, 3.45; N, 11.49; P, 15.27. Found: H, 3.40; N, 11.46; P, 15.20. Microanalyses were performed by the Microanalytical Laboratory of the Hebrew University, Jerusalem.

- (14) Dixon, N. E.; Lawrance, G. A.; Lay, P. A.; Sargeson, A. M. *Inorg. Chem.* **1983**, *22*, 847–848. The starting material was  $[(NH_3)_5RuCl]Cl_2$ , which was prepared either from  $[(NH_3)_6Ru]Cl_3$ ,<sup>15</sup> or from ruthenium trichloride.<sup>16</sup>  
 (15) Vogt, L. H.; Katz, J. L.; Wiberly, S. E. *Inorg. Chem.* **1965**, *4*, 1157–1163.  
 (16) Ferguson, J. E.; Love, J. L. *Inorg. Synth.* **1971**, *13*, 208–212.  
 (17) A  $4 \times 10^{-4}$  M complex solution in 0.1 M KH<sub>2</sub>PO<sub>4</sub> or in 0.1 M K<sub>2</sub>HPO<sub>4</sub> was titrated with either 5 M KOH or 1 M CF<sub>3</sub>SO<sub>3</sub>H. The volume changes were negligible because of the high concentration of the titrants, as indicated by the isobestic points observed: 291 nm (RuH<sub>2</sub>PO<sub>4</sub> → RuHPO<sub>4</sub> + H<sup>+</sup>); 314 and 295 nm (RuHPO<sub>4</sub> → RuPO<sub>4</sub> + H<sup>+</sup>).  
 (18) Christie, J. H.; Turner, J. A.; Osteryoung, R. A. *Anal. Chem.* **1977**, *49*, 1899–1903.  
 (19) Voltammograms and polarograms were recorded by using a homemade multipurpose polarographic analyzer and a Hewlett-Packard Model 7045B X-Y recorder. The electrochemical cell and the deaeration system were parts of a PARC automatic voltammetric electrode, Model 309.<sup>20</sup>

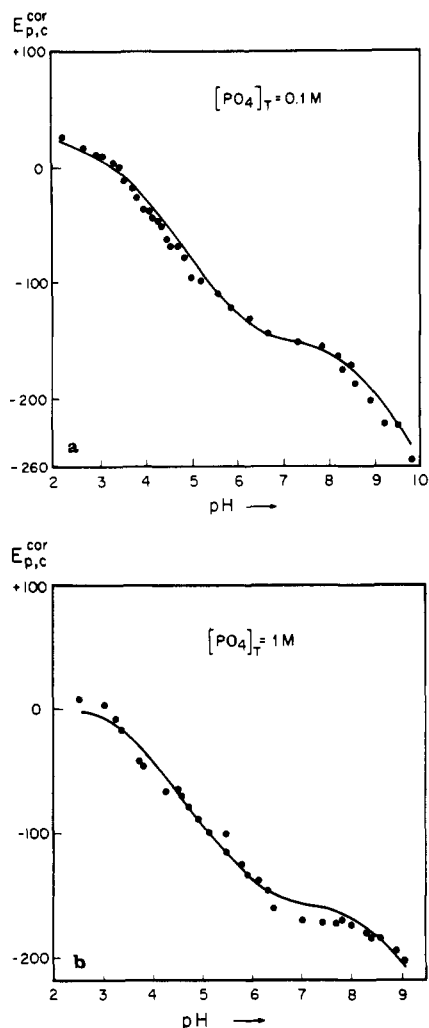


**Figure 3.** Dependence of  $E_{p,c}^{cor}$  of the  $[(NH_3)_5Ru(H_2PO_4)]^{2+/+}$  couple on pH.  $E_{p,c}^{cor}$  is the right-hand side of eq 1—the square-wave voltammetry reduction peak potential corrected for  $E_0$  and for the difference between  $E_{p,c}$  and  $E_{1/2}$  (see text): a, 0.1 M phosphate; b, 1 M phosphate.

recorded by either cyclic voltammetry or square-wave voltammetry indicated that initially only one electroactive species was present in the solution. The same conclusion is indicated by the polarographic results.

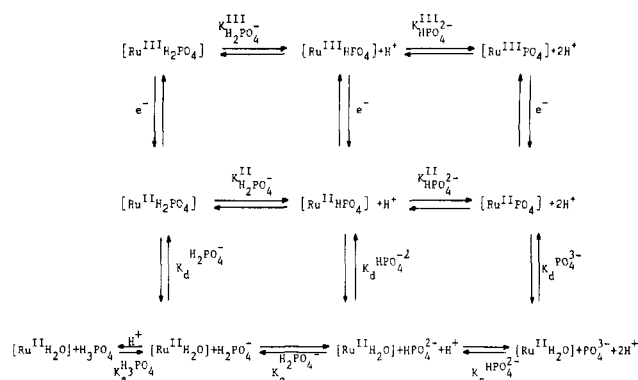
Figure 1 shows a typical cyclic voltammogram. The oxidation wave in the first scan does not correspond to the reduction wave, as indicated by the large separation between the peaks. Two peaks appear in the reduction wave of the second scan (and of later scans): the more positive peak of the two couples with the peak that appeared in the first oxidation wave, while the other peak corresponds to the original peak that appeared in the first reduction wave and has a smaller magnitude. As the scan rate is increased from 0.1 to 0.5  $V s^{-1}$ , the more positive reduction peak increases, while the second reduction peak decreases. The separation between the more positive reduction peak and the oxidation peak is 60–75 mV throughout the pH range studied. The  $E_{1/2}$  value of this couple and its pH dependence indicate that these peaks belong to the  $[(NH_3)_5Ru(H_2O)]^{3+/2+}$  couple. A  $pK_a$  of  $4.0 \pm 0.1$  could be calculated for the oxidized species, in agreement with the literature value.<sup>21</sup>

Thus, cyclic voltammetry indicates that the only species reduced in the first scan is the phosphato complex, whereas the only species oxidized is the aquo complex, which is formed from the phosphato complex after the latter is reduced. In the second scan and later, both complexes are reduced—the aquo, which was formed in the former scans, and the phosphato, which reaches the electrode by diffusion.

(20) Yarnitzky, Ch. *Anal. Chem.* **1985**, *57*, 2011–2015.

(21) Kuehn, C. G.; Taube, H. *J. Am. Chem. Soc.* **1976**, *98*, 689–702.

### Scheme I

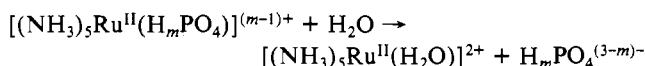


Square-wave voltammetry enables better resolution of the peaks. Figure 2 shows a typical result obtained with this method. Again, the first scan shows only one species, whereas in the second scan and later on, two species are reduced—the aquo and the phosphato.

The pH dependence of the square-wave voltammetry peak potential of the phosphato complex in 0.1 and 1 M phosphate solutions is shown in Figure 3. The pH was adjusted by adding either NaOH solution (0.01–10 M, depending on the pH and on phosphate concentration) or  $CF_3SO_3H$  (0.01 M to pure acid), dropwise, to the electrochemical cell. The initial solutions contained  $KH_2PO_4$  or  $K_2HPO_4$  in the desired concentration. The 0.1 M phosphate solutions contained 0.9 M  $CF_3SO_3Na$ , in order to obtain an ionic strength of  $\sim 1$  M.

The dependence of the potential on pH is different from what is expected, assuming a reversible reaction of the electroactive species with the electrode and taking into account the various protonation states possible and the difference in  $pK_a$  values of the complex in its different oxidation states. The dependence of  $E_{1/2}$ , which was measured by slow (0.001  $V s^{-1}$ ) polarography (at the DME), is the same, indicating that this irregular dependence is not just the result of an irreversible heterogeneous electron transfer.

The pH dependence of the potential can be explained by assuming a slow electron transfer between the electrode and the Ru(II) complex and an equilibrium



which is much faster than the electrode reaction. The slow heterogeneous electron exchange coupled with the fast ligand substitution on Ru(II) is also responsible for the fact that the only species which is oxidized is the aquo species.

The system is described fully by Scheme I, which includes the possible equilibria of the various phosphate and ruthenium-phosphato species that are present in the solution.

Figure 3 shows both the experimental results and the results calculated from eq 1, which is derived from Scheme I. This

$$E_{1/2} - E_0 = 58 \times$$

$$\log \frac{[H^+] + K_{H_2PO_4}^{II} + \frac{K_d H_2PO_4^-}{[PO_4]_T} \left( 1 + \frac{[H^+]}{K_a H_3PO_4} + \frac{K_a H_2PO_4^-}{[H^+]} \right)}{[H^+] + K_{H_2PO_4}^{III} \left( 1 + \frac{K_{HPO_4}^{III}}{[H^+]} \right)} \quad (1)$$

expression gives the rigorous value of  $E_{1/2} - E_0$  in millivolts at 20 °C. It neglects only the deprotonation of  $HPO_4^{2-}$  and of  $[(NH_3)_5Ru^{II}(HPO_4)]$ , and the protonation of  $[(NH_3)_5Ru^{II/III}(H_2PO_4)]^{+/2+}$ . These four processes are insignificant in the pH range studied.

Plots of  $E_{1/2}$  measured by polarography, and of the reduction peak potential measured by cyclic voltammetry, vs. pH are similar to the results shown in Figure 3.

**Table II.**  $pK_a$  Values for the Deprotonation of Phosphate Ions and of Water Bound to Ammine Metal Complexes and to  $H^+$ 

complex	L			
	$H_3PO_4$	$H_2PO_4^-$	$HPO_4^{2-}$	$H_2O$
$(NH_3)_5Ru^{III}L$	$\sim -1$	3.3	8.3	4.1 <sup>a</sup>
$(NH_3)_5Ru^{II}L$		6.0		13.1 <sup>a</sup>
$(NH_3)_5Co^{III}L$	-0.7 <sup>b</sup>	3.5 <sup>b</sup>	8.5 <sup>b</sup>	6.2 <sup>c</sup>
<i>cis</i> -( $NH_3$ ) <sub>2</sub> Pt <sup>II</sup> ( $H_2O$ )L		$\sim 3-3.5^d$		5.6 <sup>e</sup>
HL		2.0 <sup>f</sup>	6.9 <sup>f</sup>	
free ligand	2.0 <sup>f</sup>	6.9 <sup>f</sup>	11.7 <sup>f</sup>	

<sup>a</sup> Reference 21. <sup>b</sup> Reference 24. <sup>c</sup> Reference 25. <sup>d</sup> Estimated from ref 26. <sup>e</sup> Reference 27. <sup>f</sup> Reference 23.

The fit<sup>22</sup> between the experimental and the calculated results was obtained by changing two unknown parameters: the deprotonation constant of the phosphato complex in the Ru(II) oxidation state ( $K_{II}^{H_2PO_4^-}$ ), and the dissociation constant of  $H_2PO_4^-$  from the Ru(II) complex ( $K_d^{H_2PO_4^-}$ ). All other parameters are known from the literature (deprotonation constants of free phosphate<sup>23</sup>) or from the spectroscopic results (deprotonation constants of the Ru(III) species (vide supra) or are interrelated to the known constants by thermodynamics. The values which give the best fit are

$$K_d^{H_2PO_4^-} = 0.1 \text{ M} \quad K_{II}^{H_2PO_4^-} = 1 \times 10^{-6} \text{ M}$$

The full lines of Figure 3 represent the dependence of the right-hand side of eq 1 on pH, namely the dependence of the calculated  $E_{1/2} - E_0$  on pH. In order to compare the calculated values of  $E_{1/2} - E_0$  to the experimental values of the reduction peak potential ( $E_{p,c}$ ) of the phosphato complex, a constant value (chosen to give the best fit) was added to the experimental values. This constant corrects the measured value of  $E_{p,c}$  for  $E_0$  and for the difference between  $E_{p,c}$  and  $E_{1/2}$  of the system. The points of Figure 3 represent  $E_{p,c}^{cor}$ —the corrected values of  $E_{p,c}$ .

As Figure 3 shows, there is good agreement between the calculated and experimental results. No other set of values could reproduce the experimental results, and we estimate the accuracy of the values  $K_{II}^{H_2PO_4^-}$  and  $K_d^{H_2PO_4^-}$  as  $\pm 50\%$  from the effect of changing their values on the fit between the calculated and experimental results.

The ionic strength was almost constant in the experiments at 0.1 M phosphate: it varied slightly, from 1.0 M at pH, <6 to 1.2 M at pH >8 ( $KH_2PO_4$  present initially) or between 1.1 M at pH <6 and 1.2 M at pH >8 ( $K_2HPO_4$  present initially). In the experiments at 1 M phosphate, the ionic strength varied between 1 and 3 M ( $KH_2PO_4$  present initially) or between 2 and 3 M ( $K_2HPO_4$  present initially). The results at 1 M phosphate were identical, within the experimental error, when one started with  $K_2HPO_4$  or with  $KH_2PO_4$ . This identity together with the fact that the results at 0.1 M phosphate and at 1 M could be fitted to the calculated curves by using the same  $pK_a$  values indicates that the  $pK_a$  values do not depend significantly on the ionic strength, at least above an ionic strength of 1 M.

(22) Curve fitting was done by using an IBM-PC microcomputer and Lotus 1-2-3 software package.

(23) Smith, R. M.; Martell, A. E. "Critical Stability Constants"; Plenum Press: New York, 1976; p 56.

The results obtained at 0.01 M phosphate could not be fitted to the same scheme, either with similar values as used for the higher phosphate concentrations or with any other set of parameters. Furthermore, the electrochemical results indicate that new products are formed at this low phosphate concentration after reduction of the complex takes place. The chemistry involved is still unclear.

Table II presents the effect of coordination of  $H_2PO_4^-$  and  $HPO_4^{2-}$  to several metal centers on the  $pK_a$ 's of these ions, as well as the effect of these metal centers on the deprotonation of bound water. The effects of the metal centers on the deprotonation of bound phosphate ions parallel their effects on bound water, namely lower  $pK_a$ 's of bound water are also reflected in lower  $pK_a$ 's of the bound phosphate ions. The variation in the effects on the acidity of coordinated water is much larger than that of coordinated phosphate. The effects of the metal centers are attenuated when the site of deprotonation is separated from the metal ion by two atoms—as in the phosphate ions, as compared to water, where the oxygen from which deprotonation takes place is directly bound to the metal ion. All of the metal centers referred to in Table II enhance the acidity of phosphate due to an inductive effect, as seen by comparison with the  $pK_a$  values of the free ligand (last line in Table II). Protonation is more effective in promoting the acidity of phosphate ions than binding to any of the metal centers of Table II (compare with the  $pK_a$  values for HL- $H^+$  bound  $H_2PO_4^-$  and  $HPO_4^{2-}$ ).

The equilibrium quotient of the binding of  $H_2PO_4^-$  to  $(NH_3)_5Ru^{II}$  is  $10 \pm 5$ . That of binding to  $Co^{III}(NH_3)_5$  is 8.<sup>24</sup> The affinities of the two metal centers toward the doubly charged anion  $HPO_4^{2-}$  diverge widely:  $1.3 \times 10^4$  for the  $Co^{III}(NH_3)_5^{3+}$  center as compared to 80 for the  $Ru^{II}(NH_3)_5^{2+}$  center, both calculated from the affinity of  $H_2PO_4^-$  and the deprotonation constants of the complexed and uncomplexed ligand. The larger difference between the affinities of  $HPO_4^{2-}$  toward  $Co(III)$  and  $Ru(II)$  as compared to the difference in the affinities of  $H_2PO_4^-$  toward these two metal centers is the consequence of the higher affinity of the harder base  $HPO_4^{2-}$  (as compared to  $H_2PO_4^-$ ), toward the harder acid  $Co(III)$  (as compared to  $Ru(II)$ ).

The affinity of  $Ru(II)$  toward  $HPO_4^{2-}$  is only slightly lower than that of 2+-charged metal ions of the first transition series:  $Co^{2+}$ ,  $Ni^{2+}$ ,  $Zn^{2+}$ .<sup>28</sup> The affinity of  $Cu^{2+}$  is about 1 order of magnitude higher.<sup>28</sup>

**Acknowledgment.** This research was supported by the Technion VPR Fund-New York Metropolitan R. Fund. I thank Johnson Matthey Chemicals Ltd. for the loan of  $RuCl_3$  and Professor Ch. Yarnitzky for helpful discussions.

**Registry No.**  $[(NH_3)_5Ru(H_2PO_4)](PF_6)_2$ , 98859-01-9;  $[(NH_3)_5Ru(CF_3SO_3)](CF_3SO_3)_2$ , 84278-98-8;  $[(NH_3)_5Ru(H_3PO_4)]^{3+}$ , 98859-02-0;  $[(NH_3)_5Ru(H_2PO_4)]^{2+}$ , 98859-04-2;  $[(NH_3)_5Ru(HPO_4)]^+$ , 98859-03-1;  $(NH_3)_5Ru(PO_4)$ , 98859-00-8; zinc amalgam, 11146-96-6.

(24) Schmidt, W.; Taube, H. *Inorg. Chem.* **1963**, *4*, 698-705.

(25) Splinter, R. C.; Harris, C. J.; Tobias, R. S. *Inorg. Chem.* **1968**, *7*, 897-902.

(26) Appleton, T. G.; Berry, R. D.; Davis, C. A.; Hall, J. R.; Kimlin, H. A. *Inorg. Chem.* **1984**, *23*, 3514-3521.

(27) Basolo, F.; Pearson, R. G. "Mechanisms of Inorganic Reactions", 2nd ed.; Wiley: New York, 1967; p 32.

(28) Sigel, H.; Becker, K.; McCormick, D. B. *Biochim. Biophys. Acta* **1967**, *148*, 655-664.